TRENDS IN SCIENCES 2026; 23(1): 10976
https://doi.org/10.48048/tis.2026.10976 RESEARCH ARTICLE

Chemometric Optimization of Online SPE-LC Method Using Polypyrrole-Graphene Oxide Sorbent for Tetracycline Analysis in Water Samples

Nurzaimah Zaini[1], Ali H. Jawad[1,3,4], Nor Suhaila Mohamad Hanapi[1,2,*], Noorfatimah Yahaya[5], Ahmad Lutfi Anis[6], Sazlinda Kamaruzaman[7] and Wan Nazihah Wan Ibrahim[1,2]

[1]School of Chemistry and Environment, Faculty of Applied Sciences, Universiti Teknologi MARA, 40450 Shah Alam, Selangor, Malaysia
[2]Trace Analysis Research Group, Universiti Teknologi MARA, 40450 Shah Alam, Selangor, Malaysia
[3]Advanced Biomaterials and Carbon Development Research Group, Faculty of Applied Sciences, Universiti Teknologi MARA, 40450 Shah Alam, Selangor, Malaysia
[4]Environmental and Atmospheric Sciences Research Group, Scientific Research Center, Al-Ayen University, Thi-Qar, Nasiriyah, 64001, Iraq
[5]Integrative Medicine Cluster, Advanced Medical and Dental Institute (AMDI), Universiti Sains Malaysia, Penang 13200, Malaysia
[6]Faculty of Applied Sciences, Universiti Teknologi MARA, Kota Samarahan, Sarawak 94300, Malaysia
[7]Department of Chemistry, Faculty of Science, Universiti Putra Malaysia, Selangor 43400, Malaysia

(*Corresponding author's e-mail: norsuhaila979@uitm.edu.my)

Received: 17 June 2025, Revised: 21 July 2025, Accepted: 28 July 2025, Published: 20 October 2025

Abstract

A novel automated analytical method integrating online solid-phase extraction with liquid chromatography (online-SPE-LC) with chemometrically optimization was developed for the rapid and sensitive quantification of five selected tetracycline antibiotics, namely oxytetracycline, tetracycline, demeclocycline, chlortetracycline and doxycycline in water samples. In this method, a green polypyrrole-graphene oxide (PPy-GO) composite was employed as extraction sorbent. The effects of flow rate, valve switching time, sorbent mass, solvent composition and buffer pH were investigated using half-fraction Central Composite Design (CCD) of Response Surface Methodology (RSM). Optimal conditions were determined to be a solvent flow rate of 0.75 mL min^{-1}, valve switching time of 1.6 min, sorbent mass of 55 mg, solvent composition of 80:20 (ACN:water), and buffer pH of 2.5. The optimized method exhibited excellent linearity (R^2 = 0.9990-0.9997) across a wide concentration range (10-1000 µg L^{-1}) with low limits of detection (3.2 - 6.7 µg L^{-1}). Method precision and accuracy were demonstrated by recoveries ranging from 82% - 102% and relative standard deviations (RSDs) of 0.6% - 3.0% (*n=3*) in both river and tap water samples. Compared to existing approaches, the developed method shows superior selectivity, high sensitivity, rapid and automation. Thus, this study highlights the great potential of PPy-GO as efficient sorbent integrated with online -SPE-LC method for the extraction of tetracycline from water samples.

Keywords: Polypyrrole-graphene oxide, Online solid-phase extraction, Response surface methodology, Tetracycline antibiotics, Water samples

Introduction

Tetracycline antibiotics represent a significant number of antimicrobial agents extensively utilized in human and veterinary medicine to combat bacterial infections. Tetracyclines have extensive applications not only in clinical settings but also in agriculture for livestock treatment due to their broad-spectrum nature

and efficacy [1]. However, the impact of their pervasive use on the environment has raised concerns.

Tetracyclines are often excreted by humans and animals, entering wastewater systems directly or through manure runoff from agricultural operations [2].

Consequently, these antibiotics can accumulate in water bodies and soil, persistently existing in the environment due to their stability and resistance to degradation processes [3]. The presence of tetracycline antibiotics in aquatic environments poses significant risks on microbial populations, leading to the development of antibiotic-resistant bacteria. This resistance can spread through ecosystems and ultimately threaten the effectiveness of antibiotics in treating infections in humans and animals [4]. Studies have shown that even at low concentrations, tetracyclines can disrupt aquatic ecosystems by affecting microbial populations crucial for nutrient cycling and overall health of the ecosystem [5]. Therefore, effective mitigation strategies are essential to protect aquatic ecosystems and public health.

Liquid chromatography (LC) is widely used in laboratories for separation and analysis of complex sample matrices with precision and accuracy. Online solid-phase extraction, combined with LC, automates and simplifies sample preparation, facilitating the streamlined extraction and analysis of fluid samples directly within the chromatographic setup [6]. In online-SPE-LC setup, a specialized small SPE column and an analytical column are connected via a switching valve, allowing seamless transfer of the extracted analytes for subsequent separation and analysis [7]. Choosing the appropriate column packing material is not merely routine. It is a substantial process that relies on criteria such as the nature of the analytes, the required separation mechanism (reverse-phase, normal-phase, or ion-exchange), sample matrix, and analytical objectives [8].

Recent developments have seen graphene oxide (GO) emerging as a highly promising sorbent in modern separation technology due to its large surface area (300 - 1,500 $m^2 g^{-1}$), hydrophilicity, and abundant oxygen-containing functional groups which facilitate hydrogen bonding, π-π stacking, and electrostatic interactions with target molecules [9,10]. However, GO suffers from poor mechanical strength, tendency to agglomerate in aqueous media, and limited selectivity, which can hinder performance and reproducibility in complex matrices [11]. To overcome these drawbacks, researchers have developed composite materials incorporating GO, such as polypyrrole-graphene oxide (PPy-GO), which combine the desirable properties of GO with the versatility and chemical stability of polypyrrole (PPy) [12].

The integration of GO and PPy offers synergistic benefits in which GO contributes high surface area and active functional groups, while PPy introduces nitrogen-rich sites and prevents agglomeration. This leads to improved dispersibility, surface functionality, adsorption capacity, and selectivity for polar analytes in aqueous environments. PPy-GO has demonstrated efficiency in the removal of heavy metals [13], organic pollutants [14], and dyes [15], supporting its suitability for water treatment and analytical applications. These interactions, driven by π-π stacking and electrostatic forces, enhance its stability and utility across various sample matrices [16].

Traditional SPE methods often involve laborious sample preparation, high solvent use, limited automation, and reduced selectivity or reusability of sorbents. GO-based materials, although promising, still face the above limitations. Incorporating PPy into GO-based sorbents addresses these issues, enhancing stability and performance in aqueous matrices.

Recent advancements in online SPE systems focus on automation, rapid sample processing, and the incorporation of innovative sorbents such as magnetic nanoparticles and molecularly imprinted polymers. The use of advanced algorithms and chemometric approaches for method optimization and automated detection is gaining traction across fields like medical diagnostics and environmental monitoring [17]. While such improvements have enhanced throughput and selectivity, concerns remain regarding cost, environmental persistence, and sorbent reusability.

In this study, a chemometrically optimized online-SPE-LC method using a PPy-GO composite sorbent is proposed. This approach not only addresses the weaknesses of conventional GO-based sorbents but also integrates Response Surface Methodology (RSM) to systematically optimize extraction parameters with minimal experimental runs, improving both analytical efficiency and environmental relevance.

A half-fraction Central Composite Design (CCD) was selected over Box-Behnken Design (BBD) and full factorial design due to its ability to model linear and quadratic effects, including interactions, while minimizing the number of experimental runs. Unlike BBD, which lacks axial (star) points and is limited in detecting curvature at experimental boundaries, CCD provides more flexibility and accuracy in estimating the true response surface. Compared to full factorial design, which is less practical for multifactor optimization due to the high number of runs required, the half-fraction CCD offers a balanced trade-off between experimental economy and model predictability, making it more suitable for complex systems such as online-SPE optimization. The employment of RSM, grounded in mathematical modeling and inequality optimization, provides an efficient route to explore multi-variable interactions [18].

This study focuses on developing an extraction and separation method for tetracycline antibiotics in water using online solid-phase extraction coupled with liquid chromatography. A half-fraction CCD within RSM was employed to optimize and evaluate the interaction of key extraction parameters.

Experimental

Chemicals and materials

Five tetracycline antibiotics, namely tetracycline (TC), chlortetracycline (CTC), oxytetracycline (OTC), demeclocycline (DMC), and doxycycline (DC), each with a purity range of 98% - 101%, were sourced from Sigma-Aldrich. Graphene oxide (GO) was also acquired from Sigma-Aldrich (St. Louis, USA). Solvents, including methanol (MeOH), acetonitrile (ACN), formic acid (HCOOH), hydrochloric acid (HCl), and sodium hydroxide (NaOH), were purchased from Merck, Darmstadt, Germany. Ferric chloride hexahydrate ($FeCl_3.6H_2O$, 99.0%) and pyrrole monomer were supplied by a manufacturer in Xian, China. Ultrapure water was produced using a Barnstead Nanopure system (Thermo Scientific).

Preparation of standard and sample solutions

Individual stock solutions of OTC, TC, DMC, CTC, and DC were prepared in methanol, each at a concentration of 1,000 mg mL^{-1}. These solutions were stored in amber glass bottles at 4 °C to preserve their stability. Prior to analysis, working standard solutions were created by diluting the stock solutions in methanol to prevent analyte degradation. Tap water samples were obtained from the Environment Laboratory located at the Sarjana Building, UiTM Shah Alam, Selangor, while river water samples were collected from Sungai Segamat, Johor (coordinates: 2.5092° N, 102.8188° E), a location selected for its proximity to potential sources of pollution, including farms, veterinary clinics, and a hospital. The collected water samples were initially transported in amber bottles and kept in an icebox to ensure sample integrity. Upon reaching the laboratory, the samples were filtered using nylon membrane filters to eliminate colloidal particles before being stored at 4 °C in a freezer. For precision and accuracy testing, both the tap and river water samples, with a volume of 10 mL and a neutral pH of 7, were spiked with a standard mixture of five tetracycline antibiotics, each analyte having a final concentration of 1 mgL^{-1}.

Preparation of polypyrrole-graphene oxide (PPy-GO) composite material

The PPy-GO composite sorbent was prepared through in situ chemical polymerization of pyrrole, using a method adapted and modified from previous studies [19]. All reagents, including pyrrole monomer and $FeCl_3 \cdot 6H_2O$, were used as received without further purification. The pyrrole monomer was stored in a sealed amber vial and used immediately after opening to minimize oxidative degradation that could interfere with polymerization. Initially, 0.3 g of GO was dispersed in distilled water, creating a 3 mg mL^{-1} suspension after sonication. Following this, 250 µL of pyrrole monomer was gradually added to the GO solution under ultrasonication for 30 min. In a separate step, 0.8 g of $FeCl_3.6H_2O$ was dissolved in 10 mL of distilled water and introduced drop by drop into the mixture, followed by an additional 1 h of ultrasonication. The resulting PPy-GO composite was obtained by centrifugation, then washed several times with distilled water and ethanol. It was then dried under vacuum at 60 °C for 24 h. The dried PPy-GO powder was subsequently packed into an online SPE column for further analysis. It should be noted that although the method promotes green analytical

chemistry through reduced solvent use and automation, the synthesis of PPy-GO involves $FeCl_3$, a strong oxidant with potential environmental impact. This limitation should be addressed in future research by exploring greener alternatives for the oxidative polymerization step.

Characterization of polypyrrole-graphene oxide (PPy-GO) composite material

The physical and chemical characteristics of the synthesized PPy-GO composite sorbents were examined using various analytical techniques, including Fourier transform infrared spectroscopy (FTIR), field emission scanning electron microscopy (FESEM), x-ray diffraction (XRD), thermogravimetric analysis (TGA), and a Brunner-Emmett-Teller (BET) analyzer. Fourier transform infrared (FTIR) analysis (Thermo Fisher Scientific) was conducted using the Attenuated Total Reflection (ATR) technique with a diamond crystal, covering a spectral range of 4,000 to 400 cm^{-1}. This method allowed for the identification of functional groups, offering insights into the surface chemistry and composition of the composite through the detection of broad absorption bands. The surface morphology of the PPy-GO nanocomposite was assessed with a Zeiss Supra 40 VP FESEM at a magnification of 10,000x. XRD analysis was conducted using a PANalytical Empyrean diffractometer with copper-monochromatized (Cu-K) X-ray radiation (λ = 1.54056), set to operate at 40 kV and 40 mA, scanning from 10° to 80° at a rate of 0.0330 s^{-1}. Thermal stability was assessed by TGA (Q500, TA Instruments, USA) with approximately 5 mg of each sample heated from 100 to 500 °C at a rate of 10 °C min^{-1}. The decomposition temperature (Td) was determined from the onset of weight loss. Nitrogen adsorption and desorption isotherms were measured at –196 °C using a BELSORP-mini II instrument (BEL, Japan Inc.), with samples degassed at 70 °C for 24 h in a vacuum oven before measurement. The BET method was employed to calculate the specific surface area, total pore volume, and average pore diameter of the adsorbent.

Sorbent packing in online SPE column

The SPE column was thoroughly cleaned with DI water and rinsed with acetone prior to sorbent packing. The sorbents were immersed inside methanol solution to promote wetting, and they were slowly added using a plastic dropper into the online SPE column while the vacuum pump is on. The online SPE column was gently tapped using glass rod to ensure that the sorbents were arranged in place. This was done until the online SPE column cavity was filled with sorbent, and ready to be connected to the HPLC system. The SPE sorbent was activated by flowing methanol through the online SPE column using HPLC pump at an increasing flow rate starting from 0.1 until 1.0 mL min^{-1}. Displacement of solvent was performed using ultrapure water and acetonitrile at the same increasing flow rate.

Online solid phase extraction system

The analysis was carried out using an automated high-performance liquid chromatography (HPLC) system, specifically the Dionex Ultimate 3,000 (Sunnyvale, CA, USA). The system comprised various components, including an autosampler, dual gradient pumps on both sides, a solvent rack with a built-in vacuum degasser, a temperature-regulated column compartment, and 2 separate columns, one for online solid-phase extraction and another for analytical separation. Detection was performed using a diode array detector (DAD). For analysis, an Acclaim Polar Advantage II analytical column (5 µm, 120 Å, 4.6×150 mm) from Thermo Scientific, USA, was used, along with a C18 online SPE guard column for sample purification. A six-port programmable switching valve with two positions enabled different modes of operation. Data processing was performed using Dionex's Chromeleon™ Software, version 6.8. **Figure 1** illustrates a schematic of the online SPE-LC system, showing both the valve-switching configuration for extraction and separation, and an overview of the online SPE-LC procedure.

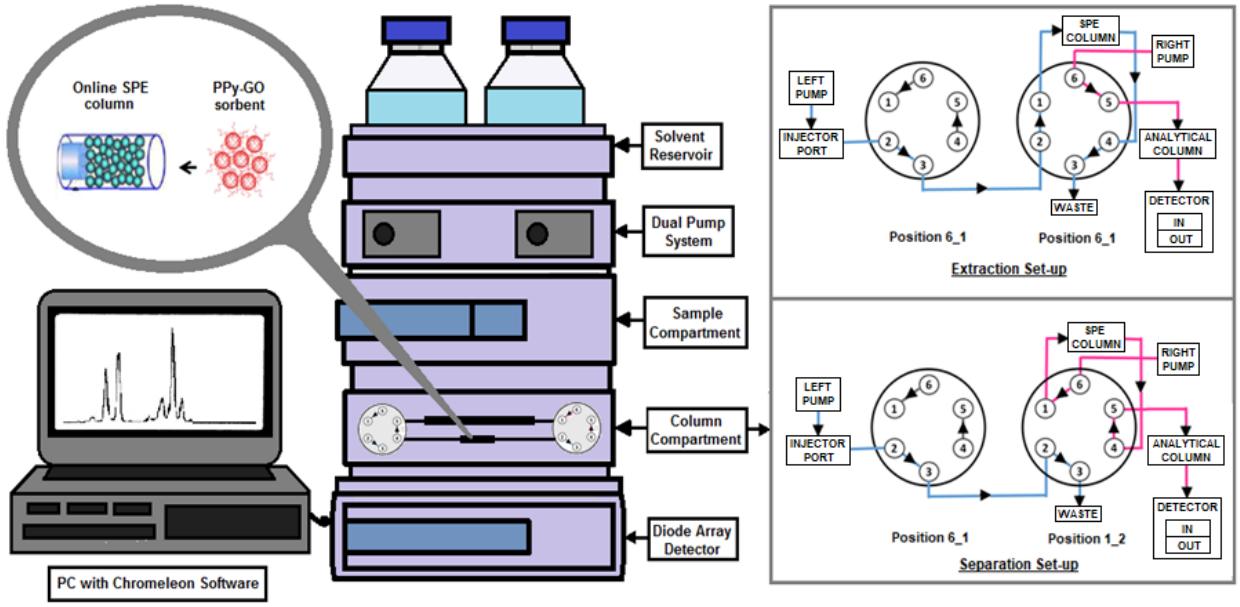

Figure 1 Schematic diagram for PPy-GO-Online-SPE-LC.

The method followed four essential steps, including sample loading, clean-up, elution, and LC separation, with both pumps operating concurrently throughout the process. During the equilibrium phase, a 10 µL spiked water sample was injected into the system *via* an autosampler, and the switching valve redirected the solvent flow to initiate sample loading. The left pump transferred the sample from the sample loop to the SPE column, while the right pump equilibrated the analytical column for separation.

To remove the sample matrix while retaining the analytes, a washing solvent was flushed through the SPE column. After the loading step, the valve was switched to the clean-up position for 1 min to remove any remaining impurities co-retained with the analytes. During the elution phase, the valve shifted to link the SPE column with the analytical column, enabling the analytes to be transported using gradient elution with the mobile phase. In the final separation phase, the valve switched back to its equilibrium mode, detaching the SPE column from the analytical column. In this phase, the right pump drove the analytes through the analytical column for separation, while the left pump equilibrated the SPE column for the next sample loading cycle.

Experimental design and statistical analysis

The experimental design was generated using Design-Expert version 13 (Stat-Ease Software) to perform regression analysis and model fitting based on the experimental data. Five key factors related to the online SPE LC method, including solvent flow rate, valve switching time, sorbent mass, solvent composition, and buffer composition, were optimized using a half-fraction central composite design (CCD) within response surface methodology (RSM). This approach was employed to enhance the extraction efficiency of tetracycline antibiotics from water samples. The experiment involved spiking ultrapure water with a standard mixture of OTC, TC, DMC, CTC, and DC at a concentration of 1 mg L^{-1}. The extraction and analysis were performed using a self-packed online SPE LC column, which contained the synthesized PPy-GO sorbent. A summary of the optimization parameters is provided in **Table 1**. The optimized conditions determined through this process were then applied to the analysis of actual water samples.

Table 1 Coded values of variables of the CCD experimental design.

Factor	Parameter	Coded Level of Variables		
		−1.00	**0**	**1.00**
A	Flow rate (mL min^{-1})	0.5	0.75	1.0
B	Valve switching time (min)	0.5	1.5	2.5
C	Sorbent mass (mg)	20	50	80
D	Solvent composition (%)	60	80	100
E	Buffer pH (pH)	2.0	2.5	3.0

Detection method

Tetracycline quantification was achieved by assessing the peak area in the chromatogram. All analytes were analyzed simultaneously with an ultraviolet/diode array detector (UV/DAD) set to a wavelength of 270 nm.

Reusability study

The reusability of the synthesized sorbent was conducted by using offline D-μ-SPE procedure starting with rinsing the sorbent five times with 2 mL methanol with sonication after each extraction. Then, the sorbent was dried at 60 °C for 1 h before further use in the next D-μ-SPE procedure. The reusability study were concluded when the percent recovery of the sorbent drops below 80%. This threshold value serves as a termination criterion for the study, indicating that the sorbent's performance has degraded significantly. The drop in percent recovery below this threshold suggests a decline in the sorbent's efficiency and may affect the reliability and accuracy of subsequent analyses.

Validation of analytical method

The developed method was evaluated for several parameters, including linearity (R^2), limit of detection (LOD), limit of quantification (LOQ), precision (% RSD), and accuracy (% recovery), before proceeding with the sample analysis. Linearity was assessed by constructing calibration curves at five different concentration levels for the tetracycline standard mixture. LOD and LOQ values were determined using matrix-matched calibration standards to closely reflect actual sample conditions. Precision was evaluated by performing three independent extractions of the calibration standard at its lowest concentration.

Results and discussion

Characterization of PPy-GO by FTIR

The spectra obtained are shown in **Figure 2**. The spectrum of GO reveals significant absorption bands corresponding to hydroxyl, carbonyl, and ether groups, indicating the presence of oxygen-containing functional groups. Specifically, bands at 3,553 cm^{-1} (O-H stretching), 1,701 cm^{-1} (C=O stretching), 1,590 cm^{-1} (C=C stretching in aromatic rings), and 1,026 cm^{-1} (C-O stretching) confirm the structural features of GO. For PPy, peaks at 3,410 cm^{-1} (N-H stretching), 2,891 cm^{-1} (C-H stretching), 1,432 cm^{-1} (C=C stretching in aromatic rings), and 1,326 cm^{-1} (C-N stretching) indicate the presence of nitrogen-containing groups and aliphatic hydrocarbons. The FTIR spectrum of the PPy-GO composite shows combined features from both GO and PPy, with shifts in peak positions suggesting interactions between the components. Notably, the hydroxyl band in GO shifts from 3,553 to 3,642 cm^{-1} and overlaps with the amine band at 3,437 cm^{-1} from PPy, indicating possible cross-linking. Other peaks, such as C-H stretching (2,904 cm^{-1}), C=O stretching (1,696 cm^{-1}), and C-N stretching (1,351 cm^{-1}), show similar but slightly shifted positions, highlighting the composite's retention of characteristic functional groups from both GO and PPy, along with new interactions or modifications. These observed shifts in FTIR peaks indicate strong molecular interactions between the GO sheets and polypyrrole chains. The shift and broadening of the hydroxyl (O-H) and amine (N-H) bands suggest the formation of hydrogen bonding or electrostatic interactions, while the changes in the C=O and C-N regions imply possible π-π stacking or charge-transfer interactions between the aromatic structures of GO and PPy. Such spectral changes are consistent with successful in situ

polymerization of pyrrole on the GO surface, confirming the formation of a stable composite material with integrated functional characteristics from both components. **Table 2** summarizes the adsorption bands that exist in the GO, PPy and PPy-GO spectra.

Table 2 Results of FTIR spectroscopy analysis of PPy-GO.

Functional Group	Wavenumbers (cm^{-1})		
	GO	PPy	PPy-GO
O-H	3553	-	3642
N-H	-	3410	3437
C-H	-	2891	2904
C=O	1701	-	1696
C=C	1590	1432	1488
C-N	-	1326	1351
C-O	1026	-	1019

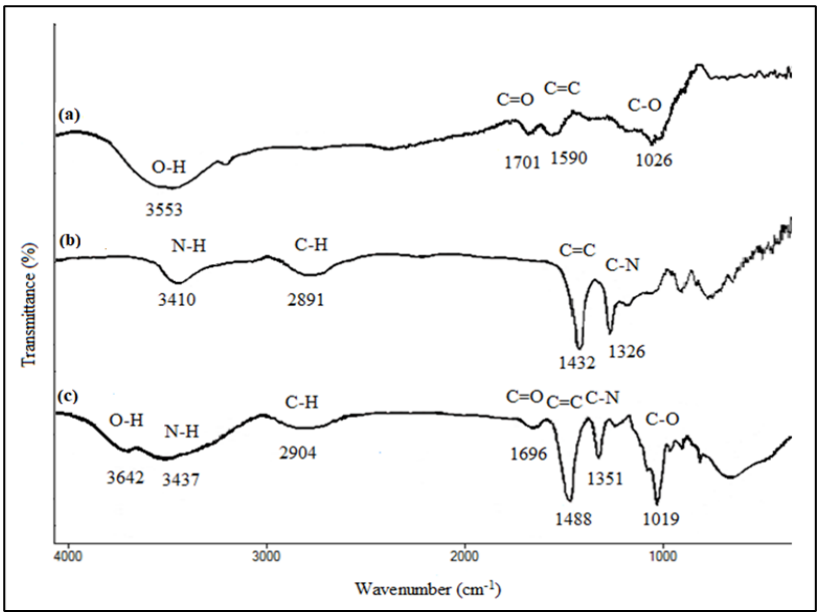

Figure 2 FTIR of (a) GO, (b) PPy and (c) PPy-GO.

Characterization PPy-GO by FESEM

Figure 3 shows the FESEM micrograph of GO, PPy and PPy-GO at 10k magnification power. The surface structure of GO in **Figure 3(a)** shows a very smooth and clear surface. The structure of PPy in **Figure 3(b),** observed under the same magnification, shows particles with an irregular, spherical shape that clump together in a random manner [20]. FESEM images of the synthesized PPy-GO composite in **Figure 3(c)** show that the segregated clumps of PPy particles are immobilized on the surface of the GO, indicating physical adsorption or possible interactions such as π-π stacking or electrostatic interactions between PPy and GO [21].

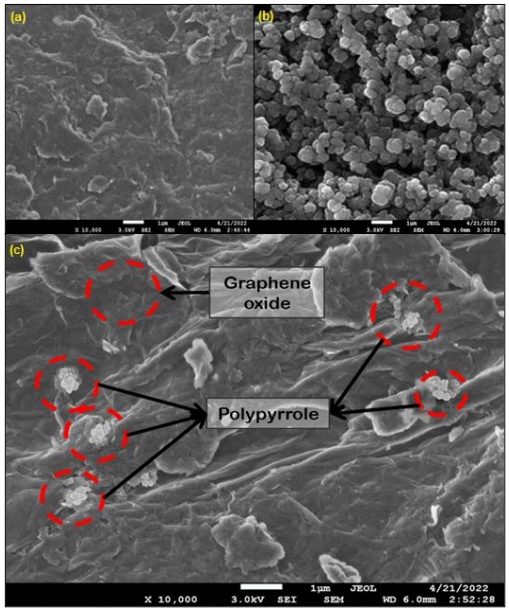

Figure 3 FESEM Micrographs of (a) GO, (b) PPy and (c) PPy-GO under 10k Magnification.

Characterization by XRD

The XRD patterns of pure PPy, GO, and the PPy-GO composite are displayed in **Figure 4**. For GO, a distinct peak is observed at 2θ = 15°, which corresponds to the (100) crystallographic plane in the graphene oxide structure. This plane is characterized by carbon-carbon bonds in a hexagonal lattice, and it is one of the prominent features of graphene-related materials. The XRD pattern obtained for pure PPy with a peak at 2θ = 26° (032), shows its semicrystalline nature [22]. The PPy-GO composite exhibits two peaks at 2θ = 10° for GO and 2θ = 26° for PPy, implying a change in the crystallographic arrangement or interplanar spacing due to the integration that occurred between the two components.

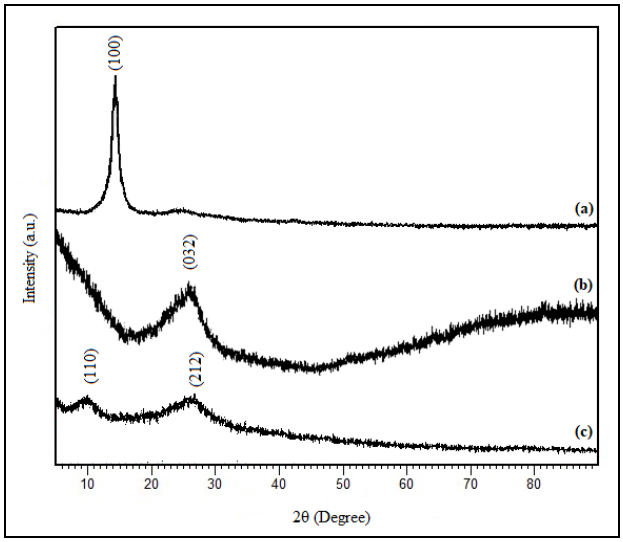

Figure 4 XRD spectrum of (a) GO, (b) PPy and (c) PPy-GO.

Thermogravimetric (TGA) analysis

Thermogravimetric analysis (TGA) profiles for PPy, GO, and PPy-GO composites are shown in **Figure 5**, highlighting their weight loss behavior across different temperature ranges. The initial weight reduction observed for all samples, from 0 to 150 °C, corresponds to moisture evaporation. The PPy sample exhibited a gradual but steady weight decrease, while the GO sample showed significant weight loss between 150 and 250 °C. This substantial reduction in the GO

weight is attributed to the decomposition of oxygen-containing functional groups present on the surface of the GO sheets. These groups are mostly eliminated during this phase, leading to the formation of single-layer graphene and expanded graphite [23].

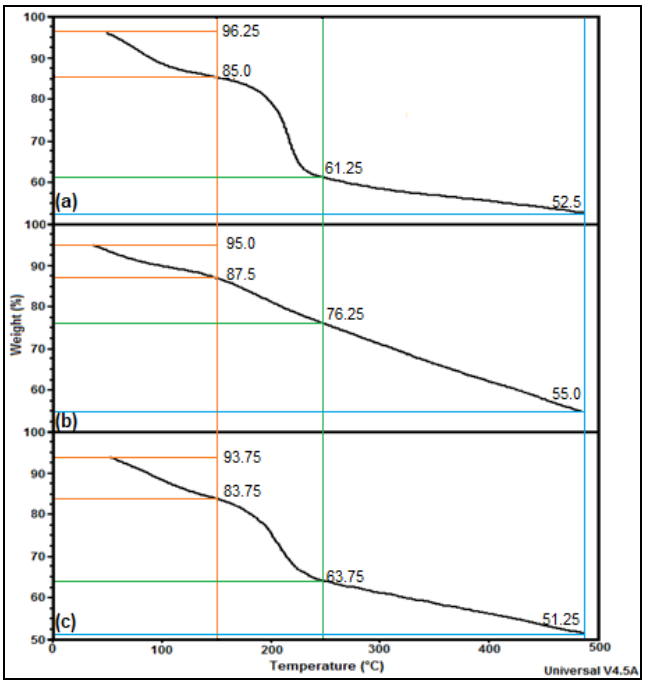

Figure 5 TGA curves of (a) GO, (b) PPy and (c) PPy-GO.

Post-thermal treatment, GO retained around 64% of its original weight, implying that the functional groups accounted for roughly 36% of its mass. For the PPy-GO composite, the initial weight loss below 150 °C is likely due to the removal of any remaining oxygen-containing functional groups, with a more significant weight loss occurring above 150 °C, potentially due to the decomposition of PPy in the composite. At 500 °C, the PPy-GO composite experienced around 50% weight loss, suggesting that half of the composite's mass remained intact at this temperature. This behavior underscores the composite's thermal stability, maintaining its structure and integrity up to 500 °C. Although TGA involves extreme temperature conditions, these results suggest that the PPy-GO composite remains stable at room temperature, making it suitable for practical applications. **Table 3** provides a summary of the weight loss percentages for GO, PPy, and PPy-GO across various temperature ranges.

Table 3 Weight loss of GO, PPy and PPy-GO at different temperatures.

Temperature (°C)	0 - 150	150 - 250	250 - 500
GO	11.25%	23.75%	8.75%
PPy	7.5%	11.25%	21.25%
GO-PPy	10.0%	20.0%	12.5%

Characterization by BET analysis

The results of the BET analysis for PPy-GO are summarized in **Table 4**, detailing its specific surface area, total pore volume, and average pore diameter. Additional BET analysis of polypyrrole and graphene oxide are provided as reference obtained from literature [24,25].

Table 4 Results for BET analysis.

Sample	PPy-GO	PPy [26]	GO [27]
BET Surface Area ($m^2 g^{-1}$)	17.087	37.1	280.7
Total Pore Volume (cc g^{-1})	0.056	0.32	0.52
Average Pore Diameter (nm)	3.390	7.82	1.21

The experimental BET surface area of the synthesized PPy-GO composite sorbent is 17.087 $m^2 g^{-1}$. Theoretically, the BET surface area for a single-layered GO sheet can reach up to 2,400 $m^2 g^{-1}$ [26]. However, real graphene samples, mainly nanoplatelets, have lower surface areas than the theoretical value [27]. In addition, the BET method may not accurately measure carbonaceous materials with large surface areas due to agglomeration [22]. The BET surface area of PPy can range from 12.4 to 211 $m^2 g^{-1}$, depending on the sample and measurement method [28]. Previous research has indicated that the BET surface area of PPy-GO composites can vary, with reported values differing between studies [29]. The total pore volume of the synthesized PPy-GO composite is 0.056 cc g^{-1}, and the average pore diameter is 3.390 nm. It was reported that hybrid polypyrrole/graphene oxide materials exhibited mixed microporous and mesoporous traits with maxima on pore size distribution profiles between 1 and 3.5 nm [29]. Combining PPy with GO may lead to a significant decrease in pore size and volume compared to pristine GO without PPy. This decrease in pore size is likely beneficial for increasing surface area, selectivity, or enhancing interactions with smaller molecules [22].

Figure 6 shows the N_2 adsorption-desorption isotherm of the PPy-GO composite material. The isotherm at 77 K indicates a Type IV hysteresis loop, suggesting a mesoporous to macroporous adsorbent with strong affinities towards adsorbate [30]. The initial part of the Type IV isotherm follows the same path as a Type II isotherm, attributed to monolayer-multilayer adsorption. The linear middle section indicates the transition from monolayer coverage to multilayer adsorption [31]. This hysteresis loop is associated with materials exhibiting capillary condensation in mesopores and macropores [32]. It is characterized by a sharp increase in adsorption at low pressures and delayed desorption at higher pressures, reflecting the desorption of adsorbate molecules from larger pores. The strong affinities suggest effective adsorption and retention of the adsorbate within the porous structure of the material, supported by chromatographic results after the extraction and separation of tetracyclines.

Despite the relatively low BET surface area observed, the sorbent exhibited strong adsorption performance in chromatographic evaluations. This suggests that other factors such as the functional surface chemistry, pore accessibility, and favorable analyte-sorbent interactions contribute significantly to extraction efficiency. The low surface area may be attributed to aggregation of GO sheets during polymerization, leading to reduced exposure of surface sites. Nonetheless, the uniform distribution of PPy over GO and the resulting mesoporous structure likely enhanced interaction with tetracycline molecules, compensating for the lower total surface area.

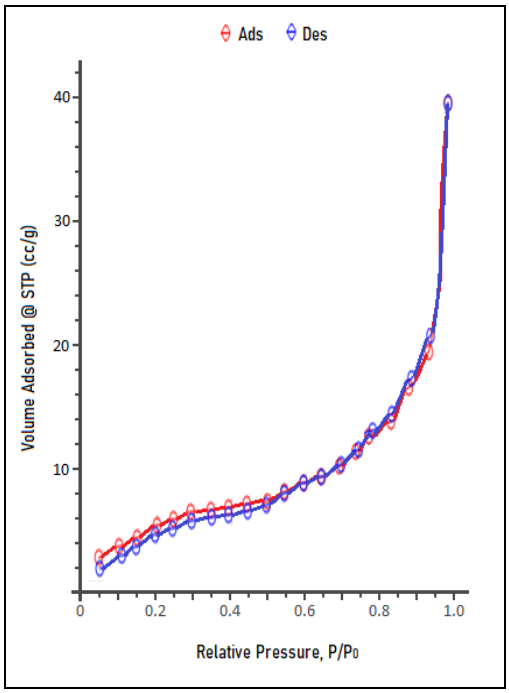

Figure 6 Specific surface area analysis (Brunauer Emmet Teller (BET) PPy-GO composite.

Point of zero charge (pHpzc)

The pH at which the overall surface charge of the particles equals zero, known as the point of zero charge (pH_{pzc}), was determined for the synthesized PPy-GO composite in this study using the salt addition method. **Figure 7** presents the pH drift data, which allowed the pHpzc value of the composite to be identified. The intersection of the ΔpH (pH_{final} - $pH_{initial}$) versus $pH_{initial}$ curve with the line where ΔpH = 0 indicated that the pH_{pzc} is approximately 4.5. This suggests that at a pH of 4.5, the composite's surface charge is neutral. When the solution pH falls below this value ($pH < pH_{pzc}$), the surface of the PPy-GO composite becomes positively charged due to the protonation of hydroxyl groups, while a higher pH results in a net negative charge [33].

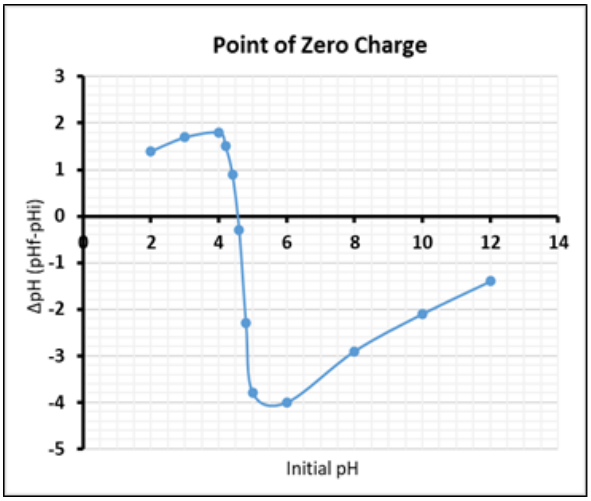

Figure 7 pH_{pzc} test of PPy-GO composite.

Optimization of extraction parameters by CCD-RSM

Five selected parameters, namely solvent flow rate, valve switching time, sorbent mass, solvent composition and buffer pH were investigated. The primary goal of employing response surface methodology (RSM) in this study is to investigate the interactions between variables and determine the key

factors that have a significant impact on the extraction efficiency of tetracyclines from water samples. A half-fraction Central Composite Design (CCD) was chosen over a full CCD and Box-Behnken Design (BBD) due to its ability to reduce the number of experimental runs while still effectively exploring the response surface [34]. This approach allowed for a more resource-efficient study without compromising the quality of the optimization process.

The interaction between the polypyrrole-graphene oxide (PPy-GO) composite sorbent and tetracycline antibiotics during extraction involves multiple adsorption mechanisms. The π-π stacking interaction between the aromatic rings of tetracycline and the conjugated system of polypyrrole facilitates the adsorption of the antibiotics onto the composite [35]. Additionally, hydrogen bonding occurs between the hydroxyl and amine groups of tetracycline and the oxygen-containing functional groups on graphene oxide, further stabilizing the composite [36]. The high surface area and porosity of the PPy-GO composite provide ample active sites for the effective adsorption of tetracycline antibiotics. **Figure 8** illustrates these proposed sorbent-sorbate interactions in detail.

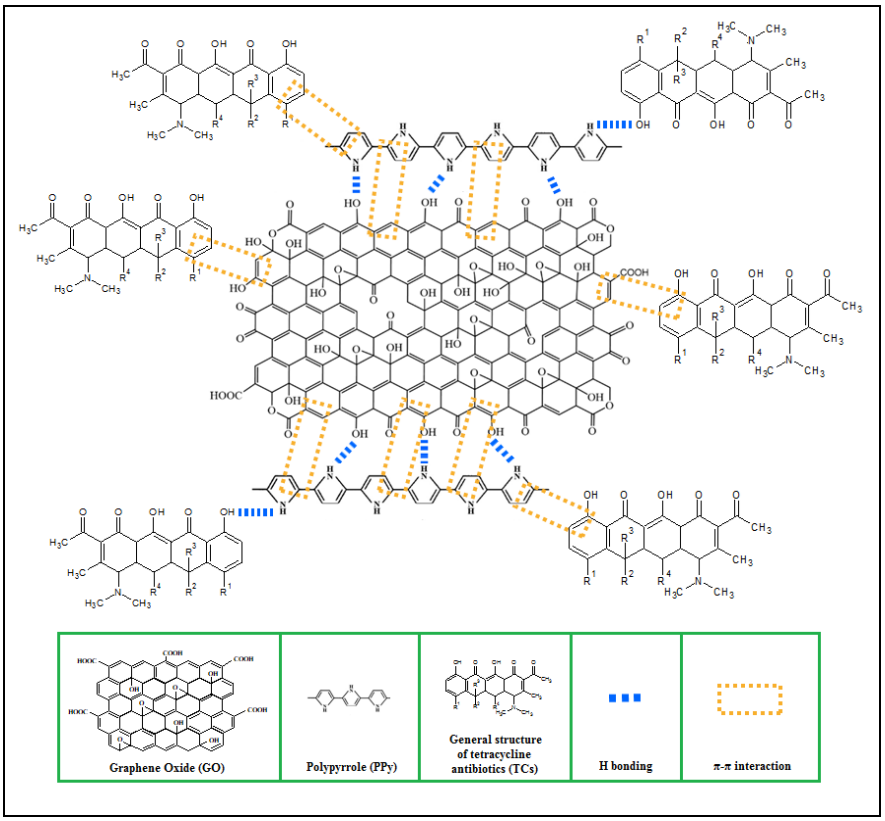

Figure 8 Possible sorbent-sorbate interactions mechanism between PPy-GO and tetracycline antibiotics during extraction.

Model fitting

The "Lack-of-Fit Tests" and model summary shown in **Table 5** compares the residual error to the "Pure Error" from replicated design points which is useful for model comparison. If there is significant lack-of-fit, as shown by a low *p*-value, then the model should be avoided to be used as a response predictor. In this case, the linear model can be ruled out, because its *p*-value falls below 0.05. The quadratic model does not show significant lack-of-fit. Robust modeling approaches supported by complex analytical methods have been instrumental in predicting system behavior and optimizing analytical performance [37]. Furthermore, it exhibits low standard deviation (Std. Dev.), high R-squared values, and a low predicted residual sum of squares (PRESS).

Table 5 Lack-of-Fit test and model summary.

Source	Sum of squares	Mean square	F-value	*p*-value	Std. Dev.	R^2	PRESS	
Linear	11344.32	540.21	602.07	< 0.0001	21.31	0.0189	1.5E+04	
2FI	10295.86	935.99	1043.17	< 0.0001	26.20	0.1095	2.3E+05	
Quadratic	28.45	4.74	5.29	0.0645	1.79	0.9972	1.2E+03	Suggested
Pure Error	3.59	0.8972						

Analysis of variance (ANOVA) and regression model analysis

The statistical significance of the model was assessed using analysis of variance (ANOVA) as shown in **Table 6**.

Table 6 ANOVA for the regression models.

Source of variation	Sum of squares	DF	Mean square	F Value	*p* Value	
Model	11534.17	20	576.708	179.986	< 0.0001	Significant
A	11.60	1	11.596	3.619	0.0863	
B	88.58	1	88.579	27.645	0.0004	
C	343.55	1	343.554	107.221	< 0.0001	
D	4.44	1	4.436	1.384	0.2666	
E	20.60	1	20.597	6.428	0.0296	
AB	35.26	1	35.255	11.003	0.0078	
AC	192.02	1	192.016	59.927	< 0.0001	
AD	179.49	1	179.492	56.018	< 0.0001	
AE	60.25	1	60.254	18.805	0.0015	
BC	63.89	1	63.886	19.938	0.0012	
BD	233.49	1	233.490	72.870	< 0.0001	
BE	7.64	1	7.637	2.383	0.1537	
CD	0.08	1	0.084	0.026	0.8750	
CE	76.71	1	76.705	23.939	0.0006	
DE	199.65	1	199.646	62.308	< 0.0001	
A^2	1787.30	1	1787.299	557.801	< 0.0001	
B^2	1665.43	1	1665.426	519.766	< 0.0001	
C^2	2375.00	1	2375.004	741.219	< 0.0001	
D^2	2009.66	1	2009.661	627.199	< 0.0001	
E^2	1922.39	1	1922.387	599.961	< 0.0001	
Residual	32.04	10	3.204			
Lack-of-Fit	28.45	6	4.742	5.285	0.0645	**Not significant**
Pure Error	3.59	4	0.897			
Cor Total	11566.21	30				

Multi-linear regression applied to the half-fraction CCD results confirmed the significance of the second-order equation for all analytes. The Model F-value of 179.99 indicates strong significance, with only a 0.01% possibility that such an F-value could occur by chance. *p*-values below 0.0500 denote significant model terms, including B, C, E, AB, AC, AD, AE, BC, BD, CE, DE, A^2, B^2, C^2, D^2, and E^2. Terms with values above 0.1000 are not significant. The lack-of-fit F-value of 5.29 suggests a 6.45% chance that this large value could be due to noise. A non-significant lack-of-fit is desirable as it indicates a well-fitting model. The high F-values and low *p*-values confirm the model's reliability. The effects of solvent flow rate, valve switching time, solvent composition, and buffer pH were evaluated using a quadratic model. The fitted regression equation for the total peak area (Y) of the analytes as a function of five variables which are solvent flow rate (A), valve switching time (B), sorbent mass (C), solvent composition (D), and buffer pH (E), is shown in Eq. 1:

$$Y = 209.04 + 0.70A + 2.18B + 4.52C + 0.43D + 0.93E - 1.48AB - 3.46AC - 3.35AD - 1.9AE - 2.00BC - 3.82BD - 0.69BE + 0.07CD - 2.19CE - 3.53DE - 7.90A^2 - 10.14B^2 - 12.14C^2 - 8.38D^2 - 8.20E^2. \quad (1)$$

In this equation, the largest positive linear coefficient is C (sorbent mass), indicating that it has the most pronounced positive effect on extraction efficiency. Conversely, the quadratic terms for C^2, B^2, and A^2 show large negative values, suggesting that increasing these factors beyond a certain point reduces performance, reflecting non-linear behavior. Interaction terms such as AC, BD, and CE also show significant negative effects, indicating that combinations of these variables may negatively impact the response if not optimized. **Table 7** presents the results for the ANOVA regression model for OTC, TC, DMC, CTC and DC. The quality of fit for the quadratic model is indicated by the R^2 value, which shows an acceptable relationship between the predicted and actual values [38].

Table 7 Summary of ANOVA analysis of TCs.

Model	Lack-of-Fit	DF	R-square	Adjusted R-square	Equation
Quadratic Significant	Not Significant	20	0.9972	0.9917	Total Peak Area = 209.04 + 0.70A + 2.18B + 4.52C + 0.43D + 0.93E – 1.48AB –3.46AC – 3.35AD – 1.9AE – 2.00BC – 3.82BD – 0.69BE + 0.07CD – 2.19CE – 3.53DE – 7.90A^2 – 10.14B^2 – 12.14C^2 – 8.38D^2 – 8.20E^2.

The R^2 value of 0.9972 and the adjusted R^2 of 0.9917, as shown in **Table 7**, indicate a well-fitted model. According to Chicco *et al.* [38], an R^2 value greater than 0.80 is considered good. The graph of predicted versus actual values in **Figure 9(a)** demonstrates a strong correlation, with points closely clustered around the diagonal line, indicating a good model fit. The average difference between actual and predicted values is less than 1.

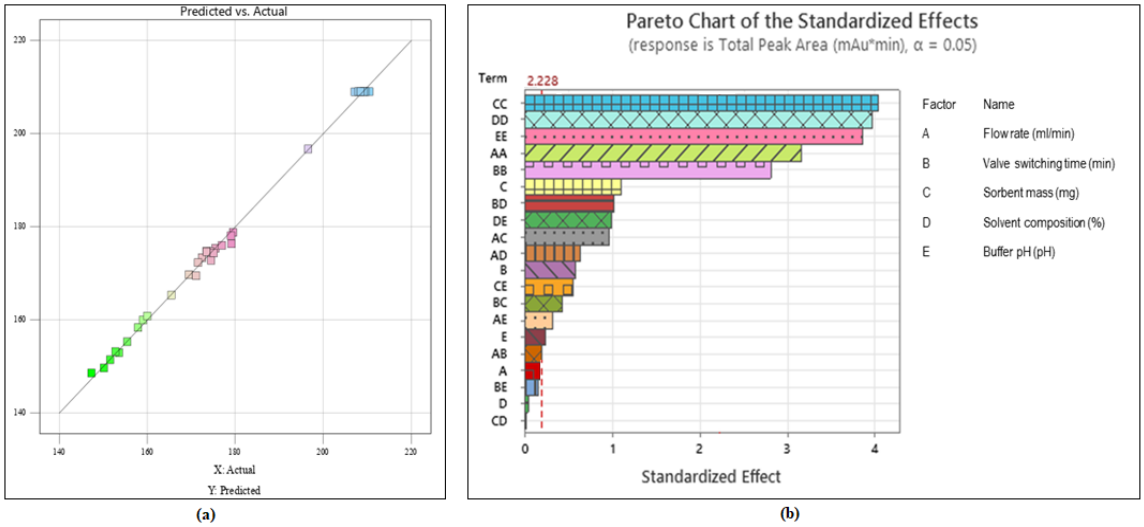

Figure 9 (a) The parity plot between predicted and actual values (b) pareto chart of the standardized effects.

The main effects of the parameters were visualized using a Pareto chart in **Figure 9(b)**. This chart displays the absolute values of standardized effects from largest to smallest, with a reference line indicating statistical significance. Bars crossing the reference line at 2.228 are significant at the $\alpha = 0.05$ level. Among the five parameters, sorbent mass is the most significant, as it directly influences extraction efficiency. Proper sorbent mass ensures effective analyte retention and minimizes losses, while insufficient or excessive sorbent mass can affect extraction performance. Balancing sorbent mass is crucial for optimal extraction conditions and improved sensitivity and precision in analytical techniques [40].

Effect of parameters on the separation of analytes

The effect of the five selected parameters can be determined by the separation of analyte's peak which can be observed from the chromatogram. The chromatogram for the three conditions of each parameter (the lowest, middle and highest condition range) were stacked together and the different in term of the appearance for all analytes, peak resolution, peak area and time taken for the first and last eluted analytes were observed. However, it should be noted that this only provides the peaks trend at that certain condition and not the optimum conditions. The optimum condition for each parameter is obtained from the optimization process of RSM in subsection 3.2.5 (Point Prediction).

Effect of valve switching time on the separation of analytes

The timing of valve switching is crucial for ensuring complete analyte extraction and successful separation. Switching the valve too soon can lead to inadequate extraction of analytes by the SPE column, which may cause poor recovery or incomplete elution of the target compounds. **Figure 10(a)** shows how valve switching time impacts analyte separation. This can be described by the online SPE valve setup shown in **Figure 10(b)**, where **Figure10(b)** illustrates extraction mode and **Figure 10(b)** shows separation mode. During extraction mode, the left pump delivers the mobile phase from the injector port to the SPE column, where the analytes are trapped by the PPy-GO sorbent, while impurities are discarded. The solvent flow in the right pump during this phase does not affect the extraction but merely the preparation for the separation step. After valve switching, the right pump moves the mobile phase to the SPE column and then to the analytical column, where the analytes are separated and detected, while the left pump prepares for the next sample.

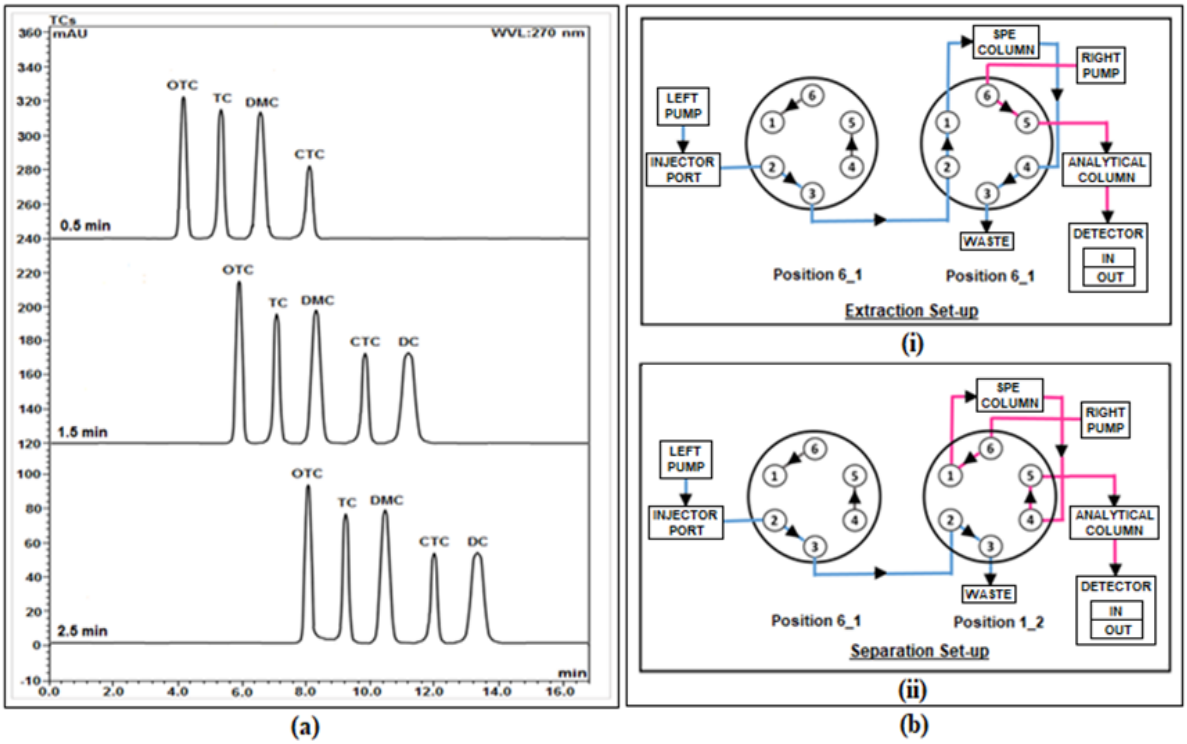

Figure 10 (a) Effect of valve switching time on the separation of analytes and (b) Online SPE valve switching Set-up for (i) Extraction mode and (ii) Separation mode.

Figure 10(a) demonstrates that at 0.5 min, only four analytes (OTC, TC, DMC, and CTC) elute within the time range, with DC missing and low CTC peak area. This suggests that the short switching time prevented full extraction [41]. At 1.5 min, all five analytes elute slightly later but are well-separated within the time range, with an additional 4 min of retention time. At 2.5 min, all analytes elute similarly to 1.5 min, but slightly later. The optimized valve switching time of 1.6 min, determined by RSM optimization, provided the highest peak area and good separation. Thus, it can be suggested that valve switching time affects peak area and retention time, but not peak resolution.

Effect of solvent composition on the separation of analytes

To optimize the solvent composition, different isocratic mixtures of acetonitrile and acidified ultrapure water (buffer) were tested, with ratios varying from 50:50 to 100:0. Increasing acetonitrile concentration speeds up analyte elution. This relationship is influenced by the polarity of both the analytes and the solvents; acetonitrile is less polar than water, so as its concentration increases, it reduces the overall polarity of the mobile phase. Analytes with lower polarity have a greater affinity for the less polar mobile phase, leading to faster elution as the solvent composition shifts toward higher acetonitrile content [42].

Figure 11(a) shows chromatograms for different solvent compositions. All five analytes were eluted at 60%, 80%, and 100% acetonitrile, but the initial peak had a slightly longer retention time at 60% compared to 80%, and 80% was slower than 100%. Higher acetonitrile concentrations resulted in shorter retention times, which is desirable for rapid analysis. **Figure 11(a)** also indicates that decreasing buffer composition while increasing acetonitrile improves separation and resolution of tetracyclines. A resolution greater than 1.5 was achieved at 60% and 80% acetonitrile. This indicates adequate separation of the analytes [43]. At 100% acetonitrile, the peaks of OTC and TC were too close, and the peak area was slightly reduced compared to 80%. Thus, 80% acetonitrile is the optimal composition, offering the best balance of peak resolution, peak area, and analysis time.

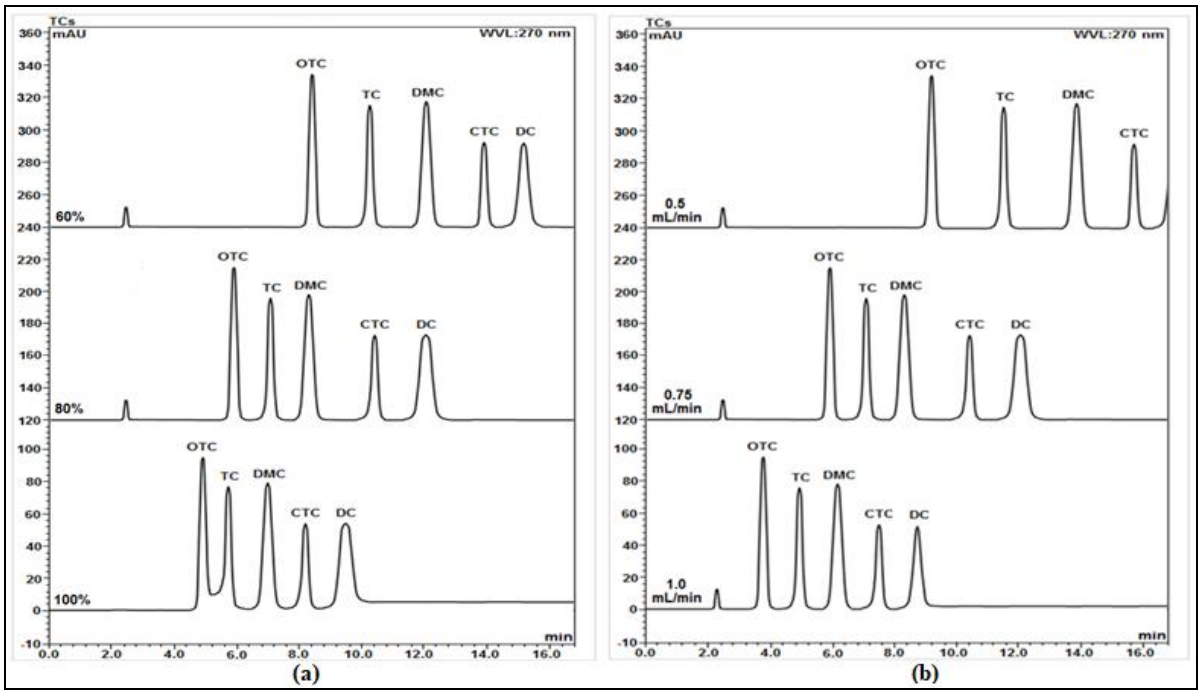

Figure 11 (a) Effect of valve switching time and (b) Solvent flow rate on the separation of analytes.

Effect of solvent flow rate on the separation of analytes

The effect of solvent flow rate on the separation of analytes within a range of 0.5 to 1.0 mL min^{-1} was investigated. This flow rate was applied throughout the entire process, including sample introduction, column washing, and analyte elution in both the extraction and separation columns. Solvent flow rate significantly affects system pressure, chromatographic quality, and analysis time [44]. While a slower flow rate may enhance separation by allowing more interaction time between the analytes and the stationary phase, it also prolongs analysis time, increases solvent usage, and may improve mass transfer efficiency by reducing band broadening, though this comes at the cost of longer run times [45]. A faster flow rate may reduce the quality of separation as the analytes have less time to interact with the stationary phase. **Figure 11(b)** shows the chromatograms for different flow rates. At 0.5 mL min^{-1}, peaks were widely spaced, with the last analyte, DC, not appearing within the standard run time, requiring an extension. In contrast, at 0.75 and 1.0 mL min^{-1}, all peaks were well separated and appeared within the time range, with only slight differences in peak area. This demonstrates that optimizing the solvent flow rate is crucial for achieving effective peak resolution and efficient analysis time.

Effect of buffer pH on the separation of analytes

A buffer solution resists changes in pH when small amounts of acid or alkali are introduced. In HPLC, a buffer maintains a consistent pH in the mobile phase, ensuring stable ionization of the analytes and reproducible retention times. The buffer stabilizes the pH, preventing fluctuations that could arise from interactions between the sample and the mobile phase, and provides the analyst with control over the pH conditions during the separation process. Tetracycline is more stable in acidic conditions than in alkaline ones [46]. The pKa values of tetracyclines indicate that these antibiotics carry localized charges across all pH levels, becoming neutral between pH 3.3 and 7.5 [47]. Below pH 3.3, Tetracyclines are positively charged, while above pH 7.5, they are negatively charged. In this study, formic acid in ultrapure water (UPW) was used as the buffer, with a pKa of 3.75. The effect of buffer pH on analyte separation was examined using formic acid concentrations ranging from 0.5 M (~pH 2) to 0.005 M (~pH 3).

As shown in **Figure 12(a)**, at pH 2.5, the analytes eluted earlier with slightly higher peaks compared to pH 2.0, where CTC and DC could not be fully separated. This lack of separation may be attributed to similarities in their chemical structures, such as pKa

values or hydrophobicity, leading to co-elution and poor resolution. Adjusting the buffer pH is therefore crucial for improving chromatographic resolution. At pH 3.0, the separation of the five analytes improved, but the peak areas for CTC and DC decreased, possibly due to ionized forms of the analytes interacting with impurities [48]. Thus, pH 2.5 emerged as the optimal buffer condition, offering the best balance between peak area and resolution.

While this study focused on a narrow pH range (2.0 - 3.0), this selection was based on the known pKa values of tetracyclines and their greater stability under acidic conditions. At pH values below 3.3, tetracyclines exist predominantly in cationic forms, promoting better interaction with the PPy-GO sorbent, which also exhibits increased positive surface charge in acidic environments. Although higher pH values (above 4.5, the estimated point of zero charge for PPy-GO) could provide additional insight into the influence of sorbent surface charge on adsorption behavior, preliminary results indicated reduced resolution and sensitivity in that region. Moreover, at basic pH, tetracyclines tend to deprotonate and become less retained. Future work should investigate this broader pH range to fully understand the interaction dynamics and expand the applicability of the method under diverse environmental conditions.

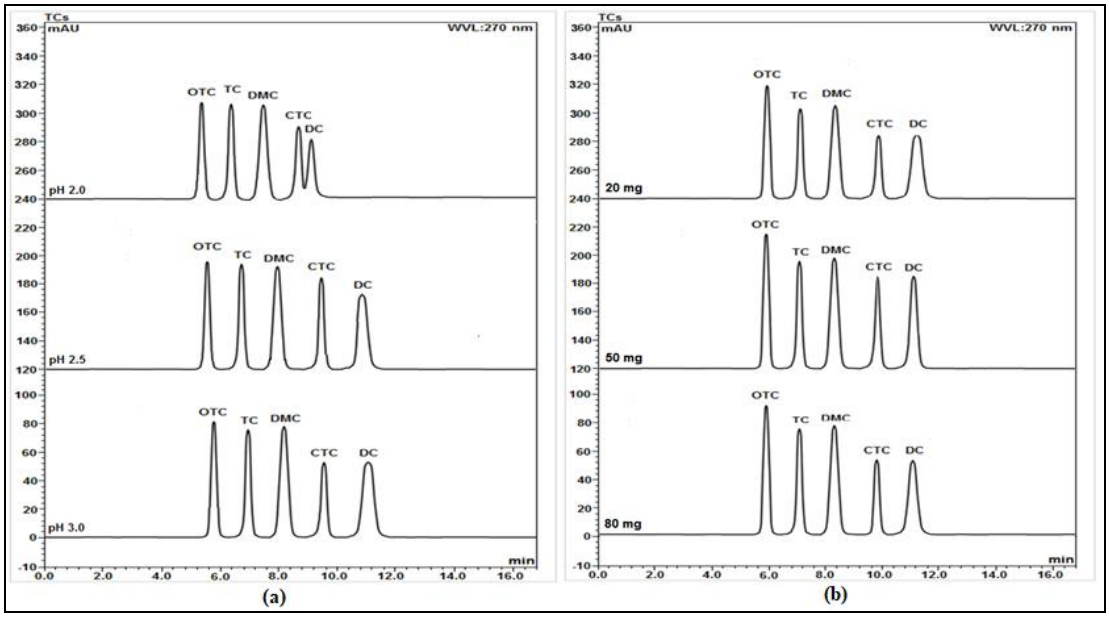

Figure 12 (a) Effect of buffer pH and (b) Sorbent mass on the separation of analytes.

Effect of sorbent mass on the separation of analytes

To achieve optimal separation of the five analytes, the effect of sorbent mass was carefully evaluated. The typical online-SPE-LC column used in this study has a 0.4 cm diameter, 5 cm length, and an internal volume of 2.51 cm^3, which can be fully packed with approximately 82.63 mg of PPy-GO sorbent. However, an experiment using a fully packed column revealed that the mobile phase was unable to pass through, likely due to the column being too tightly packed, which impeded the solvent flow [49]. As a result, an optimal sorbent mass range below the maximum capacity was explored, specifically between 20 mg and 80 mg. **Figure 12(b)** presents the chromatograms illustrating the effect of sorbent mass on analyte separation. The chromatograms show that the peaks of analytes appeared at similar retention times and with consistent peak distances across the different conditions. However, a noticeable difference was observed in peak areas, with the highest peak area recorded at 50 mg of adsorbent. This could be attributed to the mobile phase being able to flow more freely through the column, allowing better interaction between the sorbent and sorbate.

Interaction effect and respond contour plot

Figure 13 displays the interaction effects between two different parameters, with one parameter plotted on the x-axis and the total peak area on the y-axis, while the curves represent the second parameter at its minimum (black line) and maximum (red line) levels.

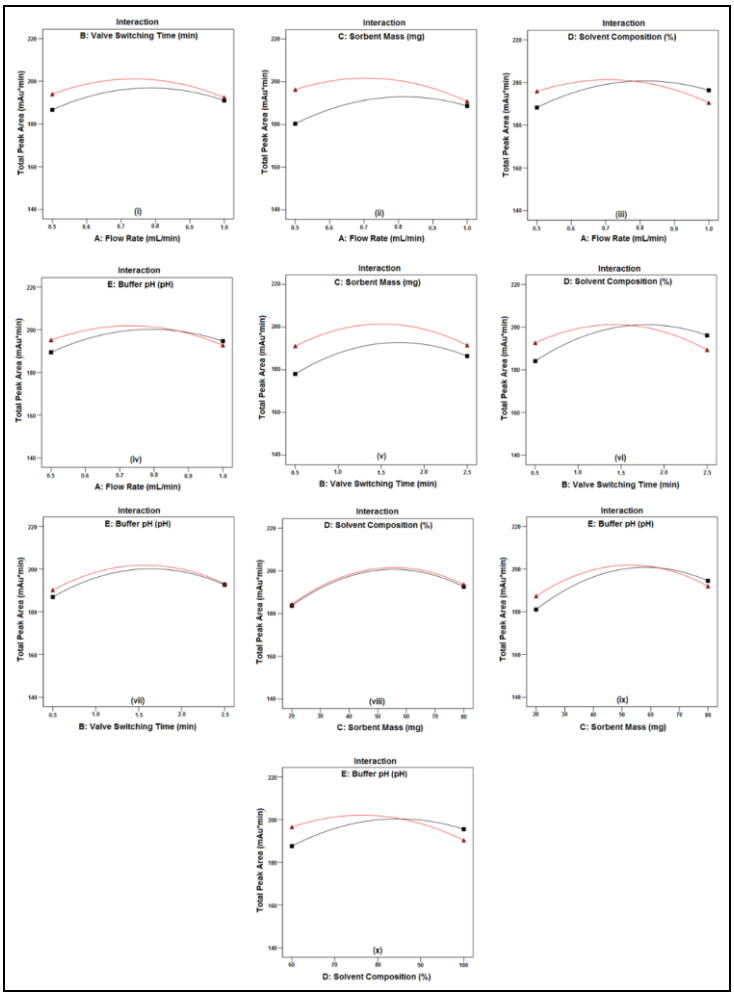

Figure 13 Graph for the Interaction effect of parameters for PPy-GO-Online SPE-LC. Legends: Black line - minimum level; red line - maximum level.

Two distinct trends can be observed from the graphs. The first trend shows that both the minimum and maximum levels of the second parameter exhibit similar patterns across the range of the first parameter. For instance, at the minimum level of the first parameter, the peak area is lower at the minimum level of the second parameter compared to its maximum level. As the first parameter increases, the peak area for both levels of the second parameter rises, reaches an optimum, and then decreases. This trend is observed in interactions such as flow rate vs. valve switching time (**Figure 13(i)**), flow rate vs. sorbent mass (**Figure 13(ii)**), and other graphs.

The second trend differs slightly, where the maximum and minimum levels of the second parameter intersect at a specific value of the first parameter, showing similar peak areas at this intersection. As the first parameter increases, the total peak area decreases, with the maximum level of the first parameter resulting in a lower peak area than the minimum level. This trend is seen in interactions such as the flow rate vs. solvent composition (**Figure 13(iii)**).

For example, **Figure 13(ii)** illustrates the interaction between flow rate (A) and sorbent mass (C). The difference in peak area between maximum and minimum sorbent mass is smaller at high flow

rates compared to low flow rates. This suggests that increasing the flow rate allows for a reduction in sorbent mass without significantly affecting the peak area.

Figure 14(i) - (x) presents the response surface plots for the parameters, namely A (solvent flow rate), B (valve switching time), C (sorbent mass), D (solvent composition), and E (buffer pH). The 3D contour plots from the model illustrate the main and interactive effects of these variables on the response [50]. Unlike interaction effect graphs, 3D contour plots do not directly show interactions but indicate that the optimal conditions for both parameters, which normally lie in the central region of their ranges, where the total peak area is maximized, as indicated by the parachute shape of the plots. For instance, **Figure 14(i)** shows the 3D contour plot of flow rate and valve switching time. From the flow rate perspective (side A), the total peak area increases with flow rate up to approximately 0.7 - 0.8 mL min^{-1}, after which it decreases. From the valve switching time perspective (side B), the total peak area increases until around 1.6 min, then decreases. Therefore, the optimal condition is where both parameters maximize the total peak area.

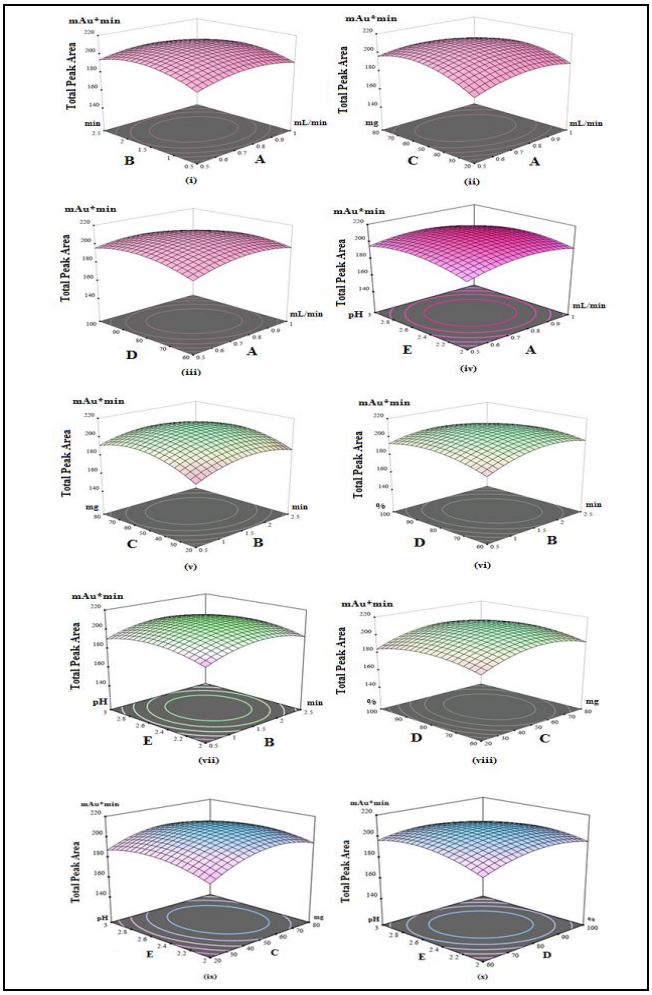

Figure 14 RSM 3-D contour plots for PPy-GO-Online SPE-LC. Legends: (A) Flow rate, (B) Valve switching time (C) Sorbent mass, (D) Solvent composition and (E) Buffer pH against peak area of analytes.

Point prediction

Based on the results obtained for the responding variable, the RSM software analyzed the data and proposed optimal conditions where all five parameters produced the highest total peak area. The optimization of the extraction process for the five selected tetracyclines using the PPy-GO-online SPE-LC method resulted in five optimal conditions: A solvent flow rate of 0.75 mL min^{-1}, a valve switching time of 1.6 min, a sorbent mass of 55 mg, an 80:20 ACN composition,

and a buffer pH of 2.5. These optimized conditions were subsequently applied to the water sample analysis.

Reusability of sorbent

The reusability study involves evaluating the ability of a material to be used multiple times without significant loss of performance or functionality [51]. In the context of an extraction sorbent, such as this PPy-GO composite, the reusability study would investigate how well the sorbent can be used for repeated cycles of extraction and recovery of target analytes. During the reusability study, the PPy-GO sorbent would be subjected to multiple extraction-desorption cycles. After each cycle, the sorbent would be regenerated or cleaned to remove any adsorbed analytes from the previous cycle. The sorbent's performance, such as its extraction efficiency, would be assessed at each cycle to determine whether it maintains consistent performance over multiple uses. The results in **Figure 15** showed that the sorbent could be conveniently reused up to fifteen times without any significant loss in the extraction recovery (> 80%) for TCs before the recovery starts to decrease slowly. This was probably due to the loss of carboxyl groups from the surface of the sorbent after repeated use [52].

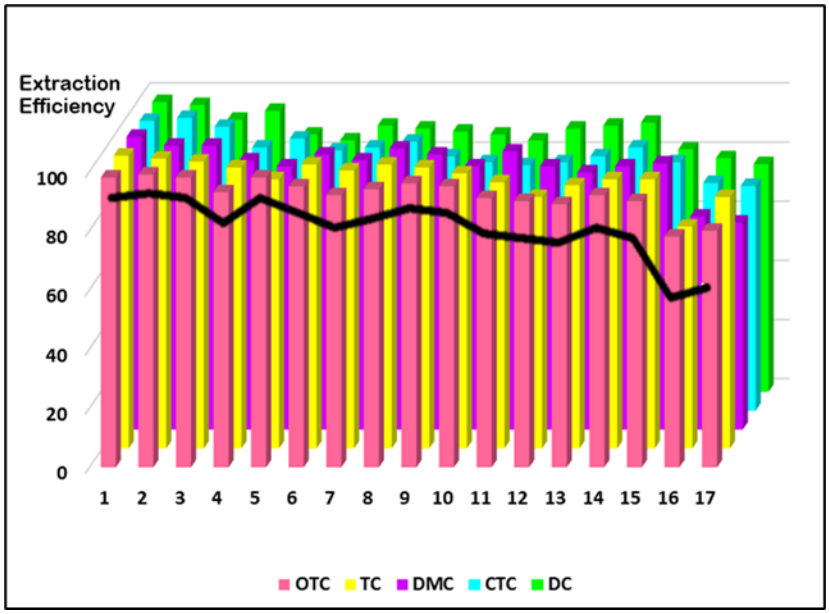

Figure 15 Reusability study.

Method validation and analytical performance of online SPE-LC

The optimized PPy-GO-based online SPE-LC method was validated in terms of linearity, sensitivity, precision, and matrix effects. Matrix-matched calibration curves were constructed in both tap water and river water matrices by spiking a standard mixture of tetracyclines at five concentration levels (10 - 1,000 μg L^{-1}) in triplicate (n = 3). **Table 8** presents the validation results, including the coefficient of determination (R^2), limits of detection (LOD), limits of quantification (LOQ), enrichment factors, and precision values for each analyte. All analytes exhibited excellent linearity, with R^2 values ranging from 0.9990 to 0.9997. The method showed good sensitivity, with LODs ranging from 3.2 to 6.7 μg L^{-1}. Precision, expressed as relative standard deviation (RSD, n = 3), was below 3.0% for all compounds in both matrices. To assess matrix effects, the slopes of calibration curves prepared in river and tap water were compared with those from standard calibration in methanol. No significant differences (within ±15%) were observed, indicating negligible matrix effects and confirming the method's reliability for application in complex environmental water samples.

Table 8 Validation data of PPy-GO-Online SPE-LC method of TCs in Tap and river water samples.

Sample	Analyte	Linear range (µg L^{-1})	Coefficient of determination R^2	LOD, (µg L^{-1})	LOQ, (µg L^{-1})	Enrichment factor	Precision (RSD, %) (*n = 3*)
Tap water	OTC	10-1000	0.9990	4.0	12.0	52	1.9
	TC	10-1000	0.9995	4.7	14.1	34	2.3
	DMC	10-1000	0.9991	5.5	16.5	31	2.5
	CTC	10-1000	0.9994	5.1	15.3	41	1.7
	DC	10-1000	0.9997	6.5	19.5	27	2.7
River water	OTC	10-1000	0.9996	3.2	9.6	45	1.9
	TC	10-1000	0.9992	4.1	12.3	30	0.6
	DMC	10-1000	0.9994	5.6	16.8	28	1.4
	CTC	10-1000	0.9996	4.9	14.7	37	3.0
	DC	10-1000	0.9997	6.7	20.1	25	2.1

Application of PPy-GO-Online-SPE-LC on river and tap water samples

A percentage recovery study was carried out by spiking river and tap water samples to achieve final concentrations of 50 and 100 µg L^{-1}. The results indicated that the recoveries were satisfactory, falling within the range of 82% to 102% (see **Table 9**). The relative recoveries obtained from both tap and river water were consistent across both concentration levels. No significant matrix-related effect was observed between the two sample types. Although river water may contain higher levels of ionic content or natural organic matter, these factors did not appear to adversely affect extraction performance. This suggests that the developed method is robust against minor matrix variations under the tested conditions. The PPy-GO-online SPE-LC method proved to be a simple, sensitive, and selective extraction method which could potentially be used in the chemical laboratory for routine analysis of water samples. **Figure 16** shows typical chromatograms of five TCs in (a) unspiked river water, (b) spiked river water, and (c) spiked tap water samples (100 µg L^{-1}) after PPy-GO-Online-SPE-LC analysis. The chromatogram demonstrated that five tetracycline antibiotics which are OTC, TC, DMC, CTC, and DC were successfully extracted and separated from both river and tap water samples, while effectively eliminating contaminants. The results affirm the successful achievement of preconcentration and clean-up through the PPy-GO-online SPE-LC method.

Table 9 Relative recoveries (%) and method precisions (RSD %, n = 3) at Two different concentrations of PPy-GO-Online SPE-LC in tap water and river water samples.

Analyte	Spiked concentration (µg L^{-1})	Tap water		River water	
		Relative Recovery (%)	RSD (%)	Relative Recovery (%)	RSD (%)
OTC	50	94	1.2	82	0.6
	500	85	1.0	85	1.7
TC	50	89	0.7	94	1.2
	500	92	1.5	101	1.5
DMC	50	87	1.1	97	3.0
	500	100	1.9	82	3.2

Analyte	Spiked concentration (µg L^{-1})	Tap water		River water	
		Relative Recovery (%)	RSD (%)	Relative Recovery (%)	RSD (%)
CTC	50	98	1.5	91	1.6
	500	95	2.1	88	2.9
DC	50	100	1.6	83	3.1
	500	86	2.0	102	3.5

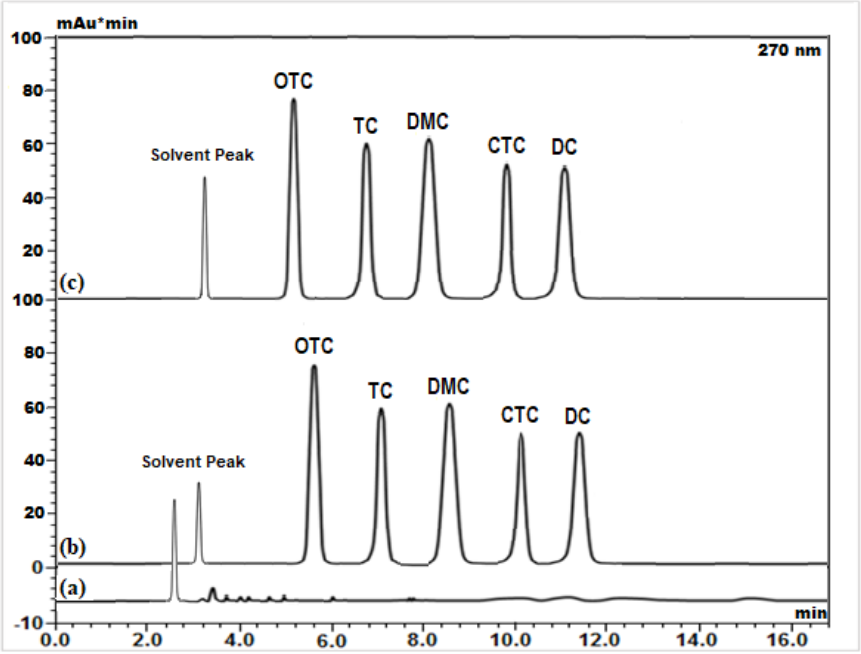

Figure 16 Typical chromatogram of five TCs in (a) unspiked river water, (b) spiked river water and (c) spiked tap water samples (100 µg L^{-1}) after PPy-GO-Online-SPE-LC analysis.

Comparison with other reported methods

The efficiency of the PPy-GO composite sorbent was compared with other reported methods, focusing on the analysis method, target analytes, and percent recovery. These comparative findings are summarized in **Table 10**. As can be seen, the method developed in this study achieved a comparable LOD with several prior reported methods. Online SPE offers significant advantages, requiring only minimal amounts of organic solvents and sorbents for each analysis, making it relatively cost-effective, straightforward, and rapid. In contrast, conventional SPE techniques often demand large quantities of organic solvents and sorbents, making the process labor-intensive, costly, and time-consuming [53]. Additionally, online SPE reduces the risk of sample contamination and human error due to its automated nature, making it more reliable and suitable for high-throughput applications.

Although the PPy-GO composite offers strong adsorption capacity and chemical stability it also provides several practical advantages over other reported materials. The composite exhibits enhanced selectivity towards tetracyclines due to the synergistic effects of π-π interactions, hydrogen bonding, and electrostatic forces provided by the functional groups on both PPy and GO. Furthermore, its synthesis is relatively simple and cost-effective, involving commonly available reagents without the need for complex functionalization or magnetic modification steps. The LODs obtained in this study (3.2 - 6.7 µg L^{-1}) are notably higher than those reported for Fe_3O_4@SiO_2@FeO MSPE-LC (0.027 - 0.107 µg L^{-1})

[54]. This variation can be attributed to differences in extraction methods and operational parameters applied in both approaches. The Fe_3O_4@SiO_2@FeO method involves an offline, magnetically-assisted microextraction that allows prolonged interaction and greater sorbent flexibility, thereby enhancing sensitivity. In contrast, the current method prioritizes full automation via online-SPE, which inherently limits sample loading volume and contact time but offers improved reproducibility, reduced manual handling, and suitability for routine analysis. Despite the difference in detection limits, the overall analytical performance and practicality of the developed method make it highly effective for environmental monitoring of tetracyclines.

The application of PPy-GO as an advanced adsorbent contributes meaningfully to several United Nations Sustainable Development Goals (SDGs), particularly SDG 3 (Good Health and Well-being), SDG 6 (Clean Water and Sanitation), and SDG 12 (Responsible Consumption and Production). Its effective removal of tetracycline antibiotics from water mitigates the risks of antimicrobial resistance and waterborne contamination, directly supporting public health and water safety initiatives [55]. Compared to bio-adsorbents, PPy-GO offers superior structural stability, reusability, and selectivity, making it more efficient in high-throughput applications and overcoming issues like limited durability or lower adsorption capacity typical of bio-based materials [56,57]. Furthermore, its synthesis and use align with circular economy principles by enabling material regeneration and reducing waste over multiple extraction cycles [58]. Overall, this material offers a sustainable and high-performance alternative for environmental remediation.

Table 10 Comparison of PPy-GO-online-SPE-LC with other previous studies for the determination of TCs in water samples.

Analysis method	Type of sample	Linear range (µg L^{-1})	LOD (µg L^{-1})	Recoveries (%)	Ref.
Fe_3O_4/aptamer-MSPE LC	Honey and water samples	10.0 to 3000.0	2.5	82.9 - 107.3	[59]
DES-based DLLME LC-UV	Well, rainforest, coastal sea	4.6 - 500	1.37 - 4.38	74 - 113	[60]
PPy-GO D-µ-SPE LC-UV/DAD	Tap, river	10 - 1000	4.9 - 8.7	80 - 105	[21]
Fe_3O_4@SiO_2@FeO MSPE LC	Tap, river	0.133 - 333	0.027 - 0.107	91.0 - 104.6	[54]
PPy-GO Online SPE-LC-UV/DAD	Tap, river	10 - 1000	3.2 - 6.7	82 - 102	This work

Abbreviation

Fe3O4/aptamer-MSPE LC: Iron(II,III)/Aptamer-Based Magnetic Solid-Phase Extraction with High-Performance Liquid Chromatography.

DES-based DLLME LC-UV: Deep Eutectic Solvent-Based Dispersive Liquid-Liquid Microextraction Liquid Chromatography with Ultraviolet Detection.

PPy-GO D-µ-SPE LC-UV/DAD: Polypyrrole-Graphene Oxide Dispersive Micro Solid-Phase Extraction Liquid Chromatography with Ultraviolet/ Diode Array Detector.

Fe3O4@SiO2@FeO MSPE LC: Ferrous Oxide Coated Magnetic Silica Magnetic Solid-Phase Extraction with High-Performance Liquid Chromatography.

PPy-GO Online SPE-LC-UV/DAD: Polypyrrole-Graphene Oxide Online Solid-Phase Extraction Coupled with Liquid Chromatography Ultraviolet Detection.

Conclusions

This study successfully developed an online solid-phase extraction combined with liquid chromatography (online-SPE-LC) method that employs polypyrrole-graphene oxide (PPy-GO) as the sorbent for analyzing five tetracycline antibiotics in water samples. The PPy-GO sorbent exhibited excellent extraction efficiency and selectivity, establishing it as a promising alternative to traditional SPE sorbents. The integration of online SPE with LC significantly enhanced extraction efficiency by reducing both extraction and analysis times. A half-fraction central composite design (CCD) of response surface methodology (RSM) was employed to investigate the interactive effects of key parameters, including flow rate, valve switching time, sorbent mass, solvent composition, and buffer pH. Among these, sorbent mass was identified as the most critical parameter, directly influencing extraction efficiency and adsorption capacity, thereby ensuring accurate, sensitive, and precise analytical results. Optimal conditions were determined to be a solvent flow rate of 0.75 mL min^{-1}, valve switching time of 1.6 min, sorbent mass of 55 mg, solvent composition of 80:20 (ACN), and buffer pH of 2.5. The method achieved excellent linearities (R^2 = 0.9990-0.9997) and limits of detection (LOD) in the range of 3.2 - 6.7 µg L^{-1}. Application to river and tap water samples yielded satisfactory relative recoveries ranging from 82% to 102%. The findings validate that the online SPE-LC method utilizing PPy-GO as sorbent is a fast, selective, and effective approach for extracting and analyzing tetracyclines in water samples. Given its automation, efficiency, and reproducibility, the method shows strong potential for real-world implementation in routine environmental monitoring programs, especially for large-scale or continuous surveillance of antibiotic contamination in water sources.

Acknowledgment

The authors would like to thank Universiti Teknologi MARA for its facilitation and knowledge support.

Declaration of Generative AI in Scientific Writing

The article was constructed using the combination of human ideas and Generative AI which are ChatGPT, Quillbot, and Mendeley. While part of the figures was created using Biorender.

CRediT Author Statement

Nurzaimah Zaini: Formal analysis, Investigation, Validation, and Writing-original draft. **Ali H Jawad:** Investigation, Validation, Review, and Visualization. **Nor Suhaila Mohamad Hanapi:** Investigation, Validation, Visualization, and Supervision. **Noorfatimah Yahaya:** Formal analysis, Investigation, Validation, and Visualization. **Ahmad Lutfi Anis:** Formal analysis, Validation, Review, and Editing. **Sazlinda Kamaruzaman:** Formal analysis, Conceptualization, and Validation. **Wan Nazihah Wan Ibrahim:** Investigation, Conceptualization, and Validation.

References

[1] F Granados-Chinchilla and C Rodriguez. Tetracyclines in food and feeding stuffs: From regulation to analytical methods, bacterial resistance, and environmental and health implications. *Journal of Analytical Methods in Chemistry* 2017; **2017(1)**, 1315497.

[2] F Ahmad, D Zhu and J Sun. Environmental fate of tetracycline antibiotics: Degradation pathway mechanisms, challenges, and perspectives. *Environmental Sciences Europe* 2021; **33**, 64.

[3] SI Polianciuc, AE Gurzau, B Kiss, MG Stefan and F Loghin. Antibiotics in the environment: Causes and consequences. *Medicine and Pharmacy Report* 2020; **93(3)**, 231-240.

[4] DG Larsson and CF Flach. Antibiotic resistance in the environment. *Nature Reviews Microbiology* 2022; **20**, 257-269.

[5] Y Amangelsin, Y Semenova, M Dadar, M Aljofan and G Bjorklund. The impact of tetracycline pollution on the aquatic environment and removal strategies. *Antibiotic*s 2023; **12(3)**, 440.

[6] D More, N Khan, RK Tekade and P Sengupta. An update on current trend in sample preparation automation in bioanalysis: Strategies, challenges

and future direction. *Critical Reviews in Analytical Chemistry* 2024; **1**, 1-25.

[7] N Zaini, NSM Hanapi, N Saim, WNW Ibrahim and AL Anis. Selective determination of acidic drugs in water samples using online solid phase extraction liquid chromatography with alginate incorporated multi-walled carbon nanotubes as extraction sorbent. *Indonesian Journal of Chemistry* 2020; **20(5)**, 987-999.

[8] ME Badawy, MA El-Nouby, PK Kimani, LW Lim and EI Rabea. A review of the modern principles and applications of solid-phase extraction techniques in chromatographic analysis. *Analytical Sciences* 2022; **38**, 1457-1487.

[9] I Reinholds, M Jansons, I Pugajeva and V Bartkevics. Recent applications of carbonaceous nanosorbents in solid phase extraction for the determination of pesticides in food samples. C*ritical Reviews in Analytical Chemistry* 2019; **49(5)**, 439-458.

[10] N Manousi, E Rosenberg, E Deliyanni, GA Zachariadis and V Samanidou. Magnetic solid-phase extraction of organic compounds based on graphene oxide nanocomposites. *Molecules* 2020, **25(5)**, 1148.

[11] JJ Guo, AM Fiore, LT Murray, DA Jaffe, JL Schnell, CT Moore and GP Milly. Average versus high surface ozone levels over the continental USA: Model bias, background influences, and interannual variability. A*tmospheric Chemistry and Physics* 2018, **18(16)**, 12123-12140.

[12] A Kaynak, A Zolfagharian, T Featherby, M Bodaghi, MP Mahmud and AZ Kouzani. Electrothermal modeling and analysis of Polypyrrole-coated wearable E-textiles. *Materials* 2021; **14(3)**, 550.

[13] S Gao, Z Liu, Q Yan, P Wei, Y Li, J Ji and L Li. Facile synthesis of polypyrrole/reduced graphene oxide composite hydrogel for Cr(VI) removal. J*ournal of Inorganic and Organometallic Polymers and Materials* 2021; **31**, 3677-3685.

[14] SNA Baharin, KP Sambasevam, NF Suhaimi, A Rahat, S Rahman and SN Musiran. Sunlight driven photocatalytic degradation of 2-chlorophenol by polypyrrole/graphene oxide composites. *Malaysian Journal of Science* 2021, **40(1)**, 67-79.

[15] S Noreen, M Tahira, M Ghamkhar, I Hafiz, HN Bhatti, R Nadeem, MA Murtaza, M Yaseen, AA Sheikh, Z Naseem and F Younas. Treatment of textile wastewater containing acid dye using novel polymeric graphene oxide nanocomposites (GO/PAN, GO/PPy, GO/PSty). *Journal of Materials Research and Technology* 2021; **14**, 25-35.

[16] M Wang, X Duan, Y Xu and X Duan. Functional three-dimensional graphene/polymer composites. *ACS Nano* 2016; **10(8)**, 7231-7247.

[17] S Sharma, RK Dubey and R Choudhary. Thermogram-based breast cancer detection using fractional derivative Sobel filtering and hybrid feature set in IoT framework. *Computational Modeling in Engineering & Sciences* 2022; **130**, 957-974.

[18] P Agarwal, SSever Dragomir, M Jleli and B Samet. *Advances in mathematical inequalities and applications*. Trends in Mathematics. Birkhauser, Switzerland, 2018.

[19] Q Sheng, D Liu and J Zheng. NiCo alloy nanoparticles anchored on polypyrrole/reduced graphene oxide nanocomposites for nonenzymatic glucose sensing. *New Journal of Chemistry* 2016; **40(8)**, 6658-6665.

[20] U Paramo-Garcia, A Avalos-Perez, J Guzman-Pantoja, NP Diaz-Zavala, JA MeloBanda, NV Gallardo-Rivas, J Reyes-Gomez, D Pozas-Zepeda, JG Ibanez and N Batina. Polypyrrole microcontainer structures and doughnuts designed by electrochemical oxidation: An electrochemical and scanning electron microscopy study. *E-Polymers* 2014; **14(1)**, 75-84.

[21] N Zaini, NSM Hanapi, WNW Ibrahim, R Osman, S Kamaruzaman, N Yahaya and AL Anis. Dispersive micro-solid-phase extraction (D-µ-SPE) with polypyrrole-graphene oxide (PPy-GO) nanocomposite sorbent for the determination of tetracycline antibiotics in water samples. *Malaysian Journal of Analytical Sciences* 2022; **26(5)**, 953-964.

[22] S Konwer, R Boruah and SK Dolui. Studies on conducting polypyrrole/graphene oxide

composites as supercapacitor electrode. *Journal of Electronic Materials* 2011; **40**, 2248-2255.

[23] J Wu, W Pisula and K Mullen. Graphenes as potential material for electronics. *Chemical Reviews* 2007; **107**, 718-747.

[24] NF Attia, SM Lee, HJ Kim and KE Geckeler. Nanoporous polypyrrole: Preparation and hydrogen storage properties. *International Journal of Energy Research* 2014; **38(4)**, 466-476.

[25] T Esfandiyari, N Nasirizadeh, M Dehghania and MH Ehrampoosh. Graphene oxide-based carbon composite as adsorbent for Hg removal: Preparation, characterization, kinetics and isotherm studies. *Chinese Journal of Chemical Engineering* 2017; **25(9)**, 1170-1175.

[26] Z Liu, Z Gao, L Xu and F Hu. Polypyrrole modified magnetic reduced graphene oxide composites: Synthesis, characterization and application for selective lead adsorption. *RSC Advances* 2020; **10(30)**, 17524-17533.

[27] S Anuma, P Mishra and BR Bhat. Polypyrrole functionalized cobalt oxide graphene (COPYGO) nanocomposite for the efficient removal of dyes and heavy metal pollutants from aqueous effluents. *Journal of Hazardous Materials* 2021; **416**, 125929.

[28] J Stejskal, M Kohl, M Trchova, Z Kolska, M Pekarek, I Krivka and J Prokes. Conversion of conducting polypyrrole nanostructures to nitrogen-containing carbons and its impact on the adsorption of organic dye. *Material Advances* 2021; **2(2)**, 706-717.

[29] A Moyseowicz and G Gryglewicz. High-performance hybrid capacitor based on a porous polypyrrole/reduced graphene oxide composite and a redox-active electrolyte. *Electrochimica Acta* 2020; **354**, 136661.

[30] P Pattananuwat, R Pornprasertsuk, J Qin and S Prasertkaew. Polypyrrole nanoparticles embedded nitrogen-doped graphene composites as novel cathode for long life cycles and high-power zinc-ion hybrid supercapacitors. *RSC Advances* 2021; **11(56)**, 35205-35214.

[31] S Kalam, SA Abu-Khamsin, MS Kamal and S Patil. Surfactant adsorption isotherms: A review. *ACS Omega* 2021; **6(48)**, 32342-32348.

[32] T Li, Z Jiang, C Xu, B Liu, G Liu, P Wang, X Li, W Chen, C Ning and Z Wang. Effect of pore structure on shale oil accumulation in the lower third member of the Shahejie formation, Zhanhua Sag, eastern China: Evidence from gas adsorption and nuclear magnetic resonance. *Marine and Petroleum Geology* 2017; **88**, 932-949.

[33] MA Gado. Sorption of thorium using magnetic graphene oxide polypyrrole composite synthesized from natural source. *Separation Science and Technology* 2018; **53(13)**, 2016-2033.

[34] T Sudha, G Divya, J Sujaritha and P Duraimurugan. Review of experimental design in analytical chemistry. *Indo American Journal of Pharmaceutical Research* 2017; **7(8)**, 550-565.

[35] M Chen, Z Yan, J Luan, X Sun, W Liu and X Ke. π-π electron-donor-acceptor (EDA) interaction enhancing adsorption of tetracycline on 3D PPY/CMC aerogels. *Chemical Engineering Journal* 2023; **454(4)**, 140300.

[36] H Sereshti, S Soltani, N Sridewi, E Salehi, E Parandi, HR Nodeh and S Shahabuddin. Solid phase extraction penicillin and tetracycline in human serum using magnetic graphene oxide-based sulfide nanocomposite. *Magnetochemistry* 2023; **9(5)**, 132.

[37] PN Sharma, G Shmueli, M Sarstedt, N Danks and S Ray. Prediction-oriented model selection in partial least squares path modeling. *Decision Sciences* 2021; **52(3)**, 567-607.

[38] D Chicco, MJ Warrens and G Jurman. The coefficient of determination R-squared is more informative than SMAPE, MAE, MAPE, MSE and RMSE in regression analysis evaluation. *Peerj Computer Science* 2021; **7(3)**, 623.

[39] M Ruzhansky, YJ Cho, P Agarwal and I Area. *Advances in real and complex analysis with applications*. Birkhauser, Switzerland, 2017.

[40] K Murtada and J Pawliszyn. Evolution in understandings of the design, optimization, and application of sorbent-based extraction devices. *TrAC Trends in Analytical Chemistry* 2023; **169**, 117396.

[41] JC Cruz, IDD Souza, CF Grecco, EC Figueiredo and MEC Queiroz. Recent advances in column switching high-performance liquid

chromatography for bioanalysis. *Sustainable Chemistry and Pharmacy* 2021; **21**, 100431.

[42] OB Rudakov, LV Rudakova and VF Selemenev. Acetonitrile as tops solvent for liquid chromatography and extraction. *Journal of Analytical Chromatography and Spectroscopy* 2023; **6**, 883.

[43] S Fekete, JL Veuthey and D Guillarme. Comparison of the most recent chromatographic approaches applied for fast and high-resolution separations: Theory and practice. *Journal of Chromatography A* 2015; **1408**, 1-14.

[44] SK Muchakayala, NK Katari, KK Saripella, H Schaaf, VM Marisetti, SK Ettaboina and VK Rekulapally. Implementation of analytical quality by design and green chemistry principles to develop an ultra-high performance liquid chromatography method for the determination of Fluocinolone Acetonide impurities from its drug substance and topical oil formulations. *Journal of Chromatography A* 2022; **1697**, 463380.

[45] SW Foster, N Wright, JP Grinias and LM Blumberg. Measurement of optimal flow rate in gradient elution liquid chromatography. *Journal of Chromatography A* 2021; **1659**, 462645.

[46] Z Li, H Jiang, X Wang, C Wang and X Wei. Effect of pH on adsorption of tetracycline antibiotics on graphene oxide. *International Journal of Environmental Research and Public Health* 2023; **20(3)**, 2448.

[47] S Casado-Terrones, A Segura-Carretero, S Busi, G Dinelli and A Fernandez-Gutierrez. Determination of tetracycline residues in honey by CZE with ultraviolet absorbance detection. *Electrophoresis* 2007; **28(16)**, 2882-2887.

[48] R LoBrutto, A Jones, YV Kazakevich and HM McNair. Effect of the eluent pH and acidic modifiers in high-performance liquid chromatography retention of basic analytes. *Journal of Chromatography A* 2001; **913(1-2)**, 173-187.

[49] JJ Kirkland and JJ DeStefano. The art and science of forming packed analytical high-performance liquid chromatography columns. *Journal of Chromatography A* 2006; **1126(1-2)**, 50-57.

[50] JP Maran, S Manikandan, B Priya and P Gurumoorthi. Box-Behnken design based multi-response analysis and optimization of supercritical carbon dioxide extraction of bioactive flavonoid compounds from tea (Camellia sinensis L.) leaves. *Journal of Food Science and Technology* 2015; **52**, 92-104.

[51] S Ncube, LM Madikizela, MM Nindi and L Chimuka. Solid phase extraction technique as a general field of application of molecularly imprinted polymer materials. *Comprehensive Analytical Chemistry* 2019; **86**, 41-76.

[52] F Wu, A Xie, M Sun, Y Wang and M Wang. Reduced graphene oxide (RGO) modified spongelike polypyrrole (PPy) aerogel for excellent electromagnetic absorption. *Journal of Materials Chemistry A* **2015**; **3(27)**, 14358-14369.

[53] I Vergara-Luis, JC Baez-Millan, I Baciero, B Gonzalez-Gaya, M Olivares, O Zuloaga and A Prieto. Comparison of conventional and dispersive solid phase extraction clean-up approaches for the simultaneous analysis of tetracyclines and sulfonamides in a variety of fresh vegetables. *Talanta* 2023; **254**, 124192.

[54] K Meftah, S Meftah, H Lamkhanter, T Bouzid, Y Rezzak, S Touil and A Abid. Extraction and optimization of *Austrocylindropuntia subulata* powder as a novel green coagulant. *Desalination and Water Treatment* 2024; **318**, 100339.

[55] S Meftah, K Meftah, M Drissi, I Radah, K Malous, A Amahrous, A Chahid, T Tamri, A Rayyad, B Darkaoui, S Hanine, O El-Hassan and L Bouyazza. Heavy metal polluted water: Effects and sustainable treatment solutions using bio-adsorbents aligned with the SDGs. *Discover Sustainability* 2025; **6**, 137.

[56] K Meftah, S Meftah, H Lamkhanter, I Hamzaoui, S Touil and A Abid. Green flocculant performance for wastewater treatment using cactus plant powder: A mini-review. *Journal of Analytical Sciences and Applied Biotechnology* 2023; **5(1)**, 29-34.

[57] S Meftah, K Meftah, H Lamkhanter, T Mehdi, A Amahrouss, F Assadid, O El Hassan and L Bouyazza. The main types of derivatives of plant matter and agricultural waste used as bio-adsorbents for the removal of heavy metals

and dyes: A review. *Egyptian Journal of Chemistry* 2024; **67(9)**, 185-207.

[58] C Tu, Y Dai, K Xu, M Qi, W Wang, L Wu and A Wang. Determination of tetracycline in water and honey by iron (II, III)/aptamer-based magnetic solid-phase extraction with high-performance liquid chromatography analysis. *Analytical Letters* 2019; **52(1)**, 1653-1669.

[59] H Sereshti, F Karami and N Nouri. A green dispersive liquid-liquid microextraction based on deep eutectic solvents doped with β-cyclodextrin: Application for determination of tetracyclines in water samples. *Microchemical Journal* 2021; **163**, 105914.

[60] L Lian, J Lv, X Wang and D Lou. Magnetic solid–phase extraction of tetracyclines using ferrous oxide coated magnetic silica microspheres from water samples. *Journal of Chromatography A* 2018; **1543**, 1-9.